Transverse Vibration Control of Axially Moving Membranes by Regulation of Axial Velocity

Quoc Chi Nguyen and Keum-Shik Hong, *Senior Member, IEEE*

***Abstract*—In this brief, a novel control algorithm that suppresses the transverse vibrations of an axially moving membrane system is presented. The proposed control method is to regulate the axial transport velocity of the membrane so as to track a desired profile according to which the vibration energy of the membrane at the end of transport decays most quickly. An optimal control problem that generates the desired profile of the axial transport velocity is solved by the conjugate gradient method. The Galerkin method is applied in order to reduce the partial differential equations describing the dynamics of the axially moving membrane into two sets of ordinary differential equations (ODEs) representing longitudinal/lateral and transverse displacements. For control design purposes, these ODEs are rewritten into state-space equations. The vibration energy of the axially moving membrane is represented by a quadratic form of the state variables. In the optimal control problem, the cost function modified from the vibration energy function is subject to the constraints on the state variables, and the axial transport velocity is considered as a control input. The effectiveness of the proposed control method is illustrated via numerical simulations.**

***Index Terms*—Axially moving membrane, conjugate gradient method, flexible electronics, Galerkin method, roll-to-roll (R2R) system, transverse vibration suppression, vibration control.**

I. Introduction

THERE are numerous industries that use web-material transport systems such as papers, textiles, metals, polymers, and composites. In these systems, the application of roll-to-roll (R2R) processing yields better performance and supports mass production and high-speed automation. However, the mechanical vibrations (particularly in the transverse direction) of web materials have been the main quality- and productivity-limiting factor, especially in high-speed R2R systems. The present work was motivated by the vibration control problem in R2R lithography systems and, indeed, it should be noted that the lithographic process is a key manufacturing technology in flexible electronics. For example, Fig. 1 depicts a R2R patterning system of Anvik Corporation [1]. In this system, the flexible substrate web, which is fed from a supply roll, extends across the exposure region on the scanning stage, and is wound onto a take-up roll. When the moving web comes to a stop, residual transverse vibrations arise naturally, even if the transport velocity of the moving web approaches the zero value. Therefore, the lithographic process has to be suspended until the web reaches a tolerable, minimal vibration state. In spite of the fact that the moving web, which is considered as an axially moving membrane, can be stabilized by the viscous damping force if the axial transport velocity is less than the critical value [2], this usually requires plenty of time. This, process delay due to the vibrations of moving materials, is a typical technical problem in almost all R2R systems. Therefore, reasonably prompt vibration suppression of moving materials for improvement of the control performance of high-speed R2R systems is desirable.

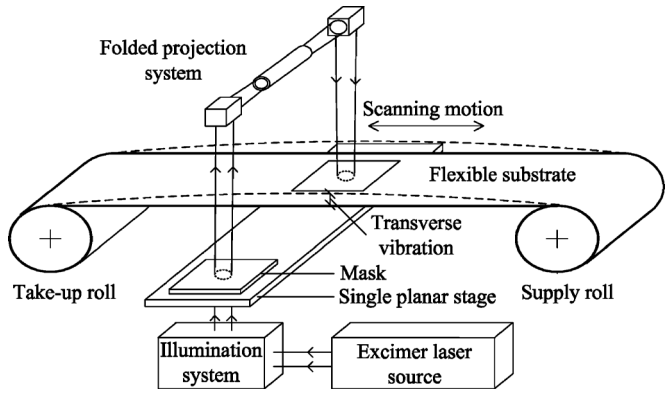

Fig. 1. Example of large-area high-throughput roll-to-roll patterning systems [1].

Vibration control schemes for axially moving systems and flexible structure systems include [3]–[22]. Boundary control techniques have been developed in [4]–[18]. These achievements were predicated on the Lyapunov energy-based method. They show that boundary control is an efficient control technique to stabilize axially moving systems. However, referring again to the practical example of the lithography R2R system, control forces exerted from boundary actuators might destroy the surface of the substrate material. Therefore, boundary control may not be a suitable solution for flexible electronics manufacturing. The distributed control method [3] is another possibility, but the disadvantage is that its implementation requires distributed sensing and/or actuation, which is impractical in flexible electronics systems. Therefore, developing a proper control method to suppress the transverse vibrations of the moving webs of flexible electronics represents a formidable challenge. This brief presents, as a means of overcoming that difficulty, a novel control algorithm that employs the effects of

Manuscript received January 19, 2011; accepted June 01, 2011. Manuscript received in final form June 06, 2011. Date of publication July 05, 2011; date of current version May 22, 2012. Recommended by Associate Editor M. Fujita. This work was supported in part by the Regional Research Universities Program (Research Center for Logistics Information Technology, LIT) and by the World Class University (Grant R31-20004) granted by the National Research Foundation of Korea under the Ministry of Education, Science and Technology, Korea.

Q. C. Nguyen is with the School of Mechanical Engineering, Pusan National University, Busan 609-735, Korea (e-mail: nqchi@pusan.ac.kr).

K.-S. Hong is with the Department of Cogno-Mechatronics Engineering and the School of Mechanical Engineering, Pusan National University, Busan 609-735, Korea (e-mail: kshong@pusan.ac.kr).

Color versions of one more of the figures in this brief are available online at http://ieeexplore.ieee.org.

Digital Object Identifier 10.1109/TCST.2011.2159384

1063-6536/$26.00 © 2011 IEEE

a time-varying axial transport velocity of the moving web to suppress transverse vibrations.

In investigating the dynamics of axially moving systems, approximation methods have been used [2], [23]–[30]. For instance, approximate solutions were obtained in [23] with the method of multiple time scales, whereas in [27], the Laplace transform method was employed. In [2], [24]–[26], and [29], the transverse displacement of an axially moving material was expanded into a Fourier series, and the Galerkin method was applied to reduce the partial differential equation (PDE) that governs the transverse motion into a set of ordinary differential equations (ODEs), which is a dimensional discrete model. It is known that the Galerkin method is quite reliable to analyze axially moving systems translating at subcritical velocities [29]. The discrete models obtained by the Galerkin method were compared with the results obtained from infinite dimensional models, and good agreements were shown in [24]–[26] and [29]. In [24], experimental results were consistent with numerical simulation results of dynamic responses of an axially moving belt using a discrete model. Indeed, the aforementioned studies have shown that the Galerkin method can be used to analyze the dynamic responses of axially moving systems.

Contributions of this brief are as follows. First, a novel open-loop control scheme for suppressing the transverse vibration of an axially moving web is presented: Contrary to the conventional methods (boundary and distributed controls) that use external forces, the proposed control method regulates the axial transport velocities of the web. Henceforth, an unexpected damage on the web surface due to external forces can be prevented. Second, the conjugate gradient (CG) method is utilized to solve an optimal control problem that generates the desired moving velocity of the web. Third, an axially moving membrane system is used to model the moving web for the first time.

II. Problem Formulation

Fig. 2 shows the axially moving membrane travelling between two fixed rolls with the time-varying axial velocity $V(t)$ in the x-direction. $V(t)$ is assumed to be smaller than the critical speed [2]. The membrane has the following geometric properties: b is the width, h is the thickness, l is the length, and $A = bl$ is the area. The material properties of the membrane are the mass density ρ, the viscous damping coefficient d_v, the Young's modulus E, and the Poisson's ratio υ. The longitudinal displacement u, the lateral displacement v, and the transverse displacement w represent the motions of the membrane in the fixed inertial frame $Oxyz$. Since u and v are in the plane of the non-deformed membrane, they are called the in-plane displacements [26]. Meanwhile, w is called the out-of-plane displacement. The displacement variables are defined as

$$u = u(x, y, t), \quad v = v(x, y, t), \quad w = w(x, y, t). \tag{1}$$

When the membrane translates with the acceleration $\dot{V}(t)$, the tension $P(x)$ of the membrane per unit width is given as [6]

$$P(x) = P_0 + \rho h x \dot{V}(t) \tag{2}$$

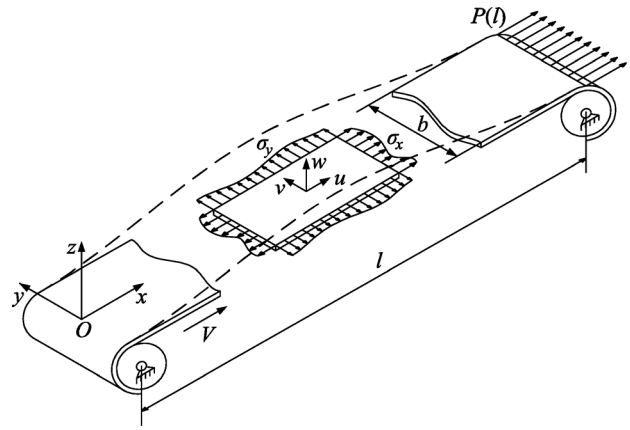

Fig. 2. Axially moving membrane travelling between two fixed rolls.

where P_0 denotes the tension of the undisturbed membrane. For notational convenience, instead of $w_x(x, y, t)$ and $w_t(x, y, t)$, w_x and w_t will be used (similar abbreviations are employed for other variables as well). According to the von Karman strain theory, the strain-displacement relations are given as [26]

$$\begin{aligned} \varepsilon_x &= u_x + w_x^2/2, \varepsilon_y = v_y + w_y^2/2 \\ \varepsilon_{xy} &= (u_y + v_x + w_x w_y)/2. \end{aligned} \tag{3}$$

The stresses are expressed as

$$\begin{aligned} \sigma_x &= Eh\,(u_x + \upsilon v_y)/(1 - \upsilon^2) \\ \sigma_y &= Eh\,(v_y + \upsilon u_x)/(1 - \upsilon^2) \\ \sigma_{xy} &= Eh\,(u_x + v_y)/2(1 + \upsilon) \\ \sigma_z &= \sigma_{xz} = \sigma_{yz} = 0 \end{aligned} \tag{4}$$

where the stresses associated with the z-direction is assumed to be zero because the thickness of the membrane is very small in comparison with other dimensions.

The kinetic energy T, the potential energy U, the virtual work done W, and the virtual the momentum transport M, respectively, are given as

$$T = \rho h \int_A \mathbf{v} \cdot \mathbf{v} dA \tag{5}$$

$$U = \int_A (\sigma_x \varepsilon_x + \sigma_y \varepsilon_y + 2\sigma_{xy}\varepsilon_{xy})\, dA \tag{6}$$

$$\begin{aligned} W = &\int_0^b (P(l)u|_{x=l} - P_0 u|_{x=0}) dy \\ &- \int_A d_v (w_t + V w_x) dA \end{aligned} \tag{7}$$

$$M = \rho h V \int_0^b \mathbf{v} \cdot \mathbf{r}|_{x=0}^{x=l}\, dy \tag{8}$$

where the displacement vector $\mathbf{r}$ and the velocity vector $\mathbf{v}$ are defined as

$$\mathbf{r} = (x + u)\mathbf{i} + (y + v)\mathbf{j} + w\mathbf{k} \tag{9}$$

$$\mathbf{v} = (V + u_t + V u_x)\mathbf{i} + (v_t + V v_x)\mathbf{j} + (w_t + V w_x)\mathbf{k} \tag{10}$$

where $\mathbf{i}, \mathbf{j}$, and $\mathbf{k}$ are the unit vectors in the x-, y-, and z-directions, respectively. Using the Hamilton's principle, the equations of motion of the axially moving membrane are derived as

$$\rho h(u_{tt} + 2Vu_{xt} + V^2 u_{xx} + \dot{V}u_x) - (\sigma_x)_x - (\sigma_{xy})_y = -\rho h\dot{V}, \tag{11}$$

$$\rho h(v_{tt} + 2Vv_{xt} + V^2 v_{xx} + \dot{V}v_x) - (\sigma_y)_y - (\sigma_{xy})_x = 0 \tag{12}$$

$$\rho h(w_{tt} + 2\dot{V}w_{xt} + V^2 w_{xx} + \dot{V}w_x) - (\sigma_x w_x + \sigma_{xy} w_y)_x - (\sigma_y w_y + \sigma_{xy} w_x)_y + d_v(w_t + Vw_x) = 0 \tag{13}$$

where the following boundary conditions are considered:

$$\sigma_x = P_0, v = w = 0, \text{ at } x = 0 \tag{14}$$

$$\sigma_x = P_0 + \rho hl\dot{V}, v = w = 0, \text{ at } x = l \tag{15}$$

$$\sigma_y = \sigma_{xy} = \sigma_y w_y + \sigma_{xy} w_x = 0, \text{ at } y = 0, b. \tag{16}$$

Remark 1: Since the stresses σ_x, σ_y, and σ_{xy} are functions of u and v, it is concluded that (11) and (12) depend on only u and v. Therefore, (11) and (12) can be solved without using (13) [26].

Remark 2: The boundary conditions (14) and (15) imply that the left and right boundaries are fixed in the sense that the vertical and lateral movements of the membrane are restricted, i.e., there is no slipping between the membrane and the rolls in the y-direction. It should be noted that the established boundary conditions are consistent with the practical example of the R2R lithography system presented in Section I.

To obtain a finite-dimensional dynamic model, the Galerkin method is applied to solve the PDEs (11)–(13). Let $\bar{u}, \bar{v}$, and $\bar{w}$ denote the weighting functions for u, v, and w, respectively. Multiplying (11)–(13) by the weighting functions and integrating the resultant equations over the area A, we obtain

$$\int_A \{\rho h\bar{u}(u_{tt} + 2Vu_{xt} + V^2 u_{xx} + \dot{V}u_x) + \rho h\bar{v}(v_{tt} + 2Vv_{xt} + V^2 v_{xx} + \dot{V}v_x) + \bar{u}_x Eh(u_x + \upsilon v_y)/(1-\upsilon^2) + \bar{v}_y Eh(\upsilon u_x + v_y)/(1-\upsilon^2) + Eh(u_y + v_x)(\bar{u}_y + \bar{v}_x)/2(1+\upsilon)\}dA = \int_0^b ((P_0 + \rho hl\dot{V})\bar{u}|_{x=l} - P_0\bar{u}|_{x=l})dy - \rho h\dot{V}\int_A \bar{u}dA \tag{17}$$

$$\int_A \{\rho h\bar{w}(w_{tt} + 2Vw_{xt} + V^2 w_{xx} + \dot{V}w_x) + \bar{w}_x(\sigma_x w_x + \sigma_{xy} w_y) + \bar{w}_y(\sigma_y w_y + \sigma_{xy} w_x) + d_v\bar{w}(w_t + Vw_x)\}dA = 0. \tag{18}$$

The displacements of the membrane are approximated by a series of suitable functions called by basis functions. Two requirements of these approximations are as follows: 1) These basis functions must be a complete set of functions and 2) the approximate functions of the displacements must satisfy the boundary conditions. Therefore, the approximate functions of the longitudinal, lateral, and transverse displacements are written in the following forms [26], respectively:

$$u(x,y,t) = \sum_{i=0}^{N}\sum_{j=0}^{N} G_{ij}^u(t) X_i(x) Y_j(y) \tag{19}$$

$$v(x,y,t) = \sum_{i=0}^{N}\sum_{j=0}^{N} G_{ij}^v(t) \sin((i+1)\pi x/l) Y_j(y) \tag{20}$$

$$w(x,y,t) = \sum_{i=0}^{N}\sum_{j=0}^{N} G_{ij}^w(t) \sin((i+1)\pi x/l) Y_j(y) \tag{21}$$

where N is the total number of the basis functions in the x- and y-directions. $G_{ij}^u(t), G_{ij}^v(t)$, and $G_{ij}^w(t)$ will be determined later. $X_i(x)$ and $Y_j(x)$ belong to the class of Legendre polynomials and are defined as

$$X_i(x) = \sum_{r=0}^{R_i} \frac{(-1)^r(2i-2r)!}{2^i r!(i-r)!(i-2r)!}(2x/l-1)^{i-2r} \tag{22}$$

$$Y_j(y) = \sum_{r=0}^{R_j} \frac{(-1)^r(2j-2r)!}{2^j r!(j-r)!(j-2r)!}(2y/l-1)^{j-2r} \tag{23}$$

where

$$R_i = \begin{cases} 1/2, & \text{if } i \text{ is even} \\ (i-1)/2, & \text{if } i \text{ is odd} \end{cases}$$
$$R_j = \begin{cases} 1/2, & \text{if } j \text{ is even} \\ (j-1)/2, & \text{if } j \text{ is odd.} \end{cases} \tag{24}$$

$\bar{u}$, $\bar{v}$, and $\bar{w}$ are expressed in the same forms as (19)–(21), where $G_{ij}^u(t), G_{ij}^v(t)$, and $G_{ij}^w(t)$ are replaced with the arbitrary functions $G_{ij}^{\bar{u}}(t), G_{ij}^{\bar{v}}(t)$, and $G_{ij}^{\bar{w}}(t)$. The finite-dimensional dynamic system will be obtained by carrying out the following procedure: (i) substituting both (19)–(21) and the weighting functions into (17) and (18), respectively; (ii) collecting all terms of the resultant equations obtained in step (i) with respect to $G_{ij}^{\bar{u}}, G_{ij}^{\bar{v}}$, and $G_{ij}^{\bar{w}}$; (iii) collecting all terms of the resultant equations obtained in step (ii) with respect to $G_{ij}^u, G_{ij}^v, G_{ij}^w, \dot{G}_{ij}^u, \dot{G}_{ij}^v, \dot{G}_{ij}^w, \ddot{G}_{ij}^u, \ddot{G}_{ij}^v$, and $\ddot{G}_{ij}^w$. A matrix-vector equation describing the dynamic state of the longitudinal and lateral displacements is obtained as

$$\mathbf{M}^{uv}\ddot{\mathbf{G}}^{uv}(t) + \mathbf{C}^{uv}(t)\dot{\mathbf{G}}^{uv}(t) + \mathbf{K}^{uv}(t)\mathbf{G}^{uv}(t) = \mathbf{O}^{uv} \tag{25}$$

where $\mathbf{G}^{uv}(t) = (G_{00}^u, G_{10}^u, \ldots, G_{NN}^u, G_{00}^v, G_{10}^v, \ldots, G_{NN}^v)^{\mathrm{T}}$. The PDE model of the transverse displacement (13) can be reduced to a set of ODEs as

$$\mathbf{M}^w\ddot{\mathbf{G}}^w(t) + \mathbf{C}^w(t)\dot{\mathbf{G}}^w(t) + \mathbf{K}^w(t)\mathbf{G}^w(t) = \mathbf{0} \tag{26}$$

where $\mathbf{G}^w(t) = (G_{00}^w, G_{10}^w, \ldots, G_{ij}^w, \ldots, G_{\mathrm{NN}}^w)^{\mathrm{T}}$. It is convenient to rewrite the ODEs (26) in the state space form as follows:

$$\dot{\mathbf{S}}(t) = \mathbf{A}(t)\mathbf{S}(t) \tag{27}$$

where

$$\mathbf{S}(t) = ((\dot{\mathbf{G}}^w(t))^{\mathrm{T}}, (\mathbf{G}^w(t))^{\mathrm{T}})^{\mathrm{T}} \tag{28}$$

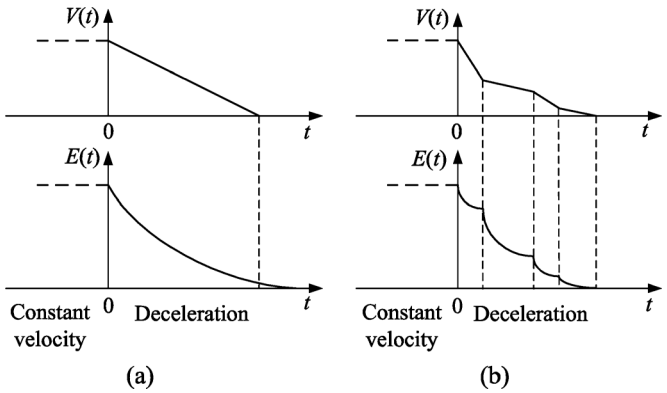

Fig. 3. Comparison of the axial velocities and the transverse vibration energies during the deceleration period. (a) Without shaping. (b) With shaping.

and

$$\mathbf{A}(t) = \begin{bmatrix} -(\mathbf{M}^w)^{-1}\mathbf{C}^w(t) & -(\mathbf{M}^w)^{-1}\mathbf{K}^w(t) \\ \mathbf{I}_{N^2\times N^2} & \mathbf{0}_{N^2\times N^2} \end{bmatrix}. \quad (29)$$

Remark 3: It follows from Remark 1 that (25) can be solved without using (26) to determine the functions $G_{ij}^u(t)$ and $G_{ij}^v(t)$, and consequently the longitudinal and lateral displacements, u and v, as well as the stresses σ_x, σ_y, and σ_{xy}. From (13), it is obvious that σ_x, σ_y, and σ_{xy} affect to the transverse displacement w. Therefore, the determined functions of these stresses will be used to obtain the approximate solution of w through (26).

Remark 4: In practice, since the length l is much larger than the width b and the thickness h, the in-plane stiffness is much higher than the out-plane stiffness. Therefore, it can be assumed that u and v are very small in comparison with w. Based on this assumption, in this brief, only suppression of the transverse displacement is focused.

Remark 5: For control design purposes, the linear operator $\mathbf{A}$ combined with the approximate solution (21) will be used to describe the dynamics of the transverse displacement. It is obvious that the matrices $\mathbf{C}^w(t)$ and $\mathbf{K}^w(t)$, and consequently $\mathbf{A}(t)$, are functions of $V(t)$. This allows the eigenvalues of $\mathbf{A}$ as well as the convergence speed, when $\mathbf{S}(t) \to 0$, to be adjusted by changing $V(t)$. Upon such a technical basis, a control algorithm that utilizes the effects of the axial transport velocity to suppress the transverse vibration is developed.

III. Control Design

Fig. 3 illustrates the idea of the proposed control algorithm. In the case of no control, the axial transport velocity is regulated to decrease from $V(0)$ to zero using the conventional profile constructed from a slope; that is, the transport deceleration is constant. The conventional constant-deceleration profile shown in Fig. 3(a) is a typical example widely used in practice. In this case, the vibration energy $E(t)$ tends naturally to zero in the presence of viscous damping. However, the phenomenon that the residual vibration energy still has considerable value when the axial transport velocity arrives at zero usually occurs. Moreover, the convergence of $E(t)$ to zero depends on the value of the viscous damping coefficient of the web material. Therefore, vibration suppression that relies only on the viscous damping force usually requires plenty of time. As shown in Fig. 3(b), when the developed control algorithm is applied, the axial transport velocity is regulated to track a profile constructed from several slopes instead of the conventional constant-deceleration profile. This control algorithm is expected to impart two improvements to control performance. First, the vibration energy is expected to decay quickly. Second, when the axial transport velocity reaches the zero value, the transverse vibration is suppressed completely. These improvements were validated both by theoretical calculations [see (39)(40)–(53)] and numerical simulation results. To obtain the proposed profile, an optimal control problem is established, in which the cost function is modified from the vibration energy function of the membrane system and the time-varying axial transport velocity is considered as a control input. The CG method [31], [32] was used to solve the optimal control problem. The application of the CG method provides a good convergence property for the cost function as well as the vibration energy. As shown in Fig. 4, the vibration energy of the moving web tends to the minimum point (the zero value) in a zigzag fashion; that is, in every iteration of the CG algorithm, $V(t)$ is regulated so that $E(t)$ decreases in the direction opposite to the gradient of $E(t)$, where $E(t)$ decreases most quickly.

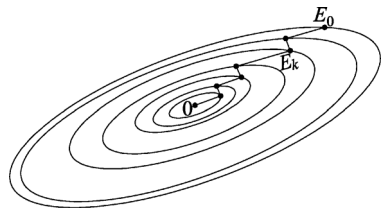

Fig. 4. Convergence of the vibration energy in zigzag fashion.

The state-space model (27) is rewritten as

$$\begin{aligned}\dot{\mathbf{S}}(t) &= \mathbf{F}(\mathbf{S}, V, \dot{V}) \\ &= \mathbf{A}_c\mathbf{S}(t) + V(t)\mathbf{B}_1\mathbf{S}(t) + V^2(t)\mathbf{B}_2\mathbf{S}(t) \\ &\quad + d_v V(t)\mathbf{B}_3\mathbf{S}(t) + \sigma_x\mathbf{B}_4\mathbf{S}(t) \\ &\quad + \sigma_y\mathbf{B}_5\mathbf{S}(t) + \sigma_{xy}\mathbf{B}_6\mathbf{S}(t) \end{aligned} \quad (30)$$

where $V(t)$ is considered as a control input. In this brief, since the function describing the axial transport velocity is assumed to be piecewise linear in every iteration of the CG algorithm, that is, $\dot{V}$ is a constant, $\mathbf{A}_c$ and $\mathbf{B}_i (i = 1, \ldots, 6)$ are constant matrices.

The vibration energy of the membrane system, in which only the transverse vibration is focused, is represented as

$$\begin{aligned} E(t) &= \frac{1}{2}\int_A \rho h(w_t + Vw_x)^2 dA \\ &\quad + \frac{1}{2}\int_A \left(\sigma_x w_x^2 + \sigma_y w_y^2 + 2\sigma_{xy} w_x w_y\right) dA. \end{aligned} \quad (31)$$

From (22) and (23), the following inequalities are obtained:

$$|X_i(x)| < \sum_{r=0}^{R_i} \frac{(2i-2r)!}{2^i r!(i-r)!(i-2r)!} \quad (32)$$

$$|(X_i(x))_x| < \sum_{r=0}^{R_i} (2(i-2r)/l) \frac{(2i-2r)!}{2^i r!(i-r)!(i-2r)!} \quad (33)$$

$$|Y_j(y)| < \sum_{r=0}^{R_j} \frac{(2j-2r)!}{2^j r!(j-r)!(j-2r)!} \tag{34}$$

$$|(Y_j(y))_y| < \sum_{r=0}^{R_j} (2(j-2r)/b) \frac{(2j-2r)!}{2^j r!(j-r)!(j-2r)!}. \tag{35}$$

Substituting (19)–(21) into (31) and using the inequalities (32)–(35), the vibration energy (31) is then evaluated as

$$\begin{aligned} E(t) \le \frac{\rho hbl}{2} & \left(\sum_{i=0}^{2N^2} \xi_1 (1 + \psi(i)(i - N^2 + 1)\pi V/l) S_i \right)^2 \\ & + \xi_3 bl \left(\sum_{i=0}^{2N^2} (\xi_1 \psi(i)(i - N^2 + 1)/l) S_i \right)^2 \\ & + \xi_4 bl \left(\sum_{i=0}^{2N^2} (\xi_2 (i - N^2 + 1)\pi/l)\psi(i) S_i \right)^2 \\ & + \xi_5 bl \left(\sum_{i=0}^{2N^2} \xi_2 \psi(i) S_i \right)^2 \end{aligned} \tag{36}$$

where the Heaviside step function $\psi(i)$ is defined as

$$\psi(i) = \{\mathrm{sgn}(i - N^2) + |\mathrm{sgn}(i - N^2)|\}/2 \tag{37}$$

and $\xi_i (i = 1, \ldots, 5)$ are positive constants. The upper bound of the vibration energy (31) is obtained as

$$\bar{E}(t) = \frac{1}{2} \mathbf{S}^{\mathrm{T}}(t) \mathbf{Q}(t) \mathbf{S}(t) \tag{38}$$

where $\mathbf{Q}$ is a positive symmetric matrix of size $2N^2 \times 2N^2$.

Remark 6: It should be noted that if $\bar{E}(t)$ converges to zero, $E(t)$ also converges to zero. From (38), it is obvious that $\bar{E}(t)$ is represented in a linear quadratic form, which is a convenient form for application of the CG method. Therefore, $\bar{E}(t)$ will be used to establish the optimal control problem.

To solve the optimal control problem is to find the axial transport velocity $V(t)$ that minimizes the cost function

$$J(t_f) = \frac{1}{2} \mathbf{S}^{\mathrm{T}}(t_f) \mathbf{Q}(t_f) \mathbf{S}(t_f) \tag{39}$$

where t_f is the terminal time, subject to the state-space equations (30) with the initial and final conditions of the state vector

$$\mathbf{S}(0) = \mathbf{S}_0 \tag{40}$$

$$\mathbf{S}(t_f) = \mathbf{0} \tag{41}$$

and subject to the inequality constraint of the control input

$$V(t) > 0. \tag{42}$$

The initial state $\mathbf{S}(0) = \mathbf{S}_0$ can be obtained from the initial conditions

$$w(x, y, 0) = w_0(x, y),\ w_t(x, y, 0) = w_{t0}(x, y). \tag{43}$$

The constraint (41) is combined with the cost function (39) as

$$\tilde{J}(t_f) = \frac{1}{2} \mathbf{S}^{\mathrm{T}}(t_f) [\mathbf{Q}(t_f) + \mathbf{W}] \mathbf{S}(t_f) \tag{44}$$

where $\mathbf{W}$ is a weight coefficient matrix of size $2N^2 \times 2N^2$. From (30), since $V(t)$ is piecewise linear in every iteration of the CG algorithm, the function $\mathbf{F}(\mathbf{S}, V, \dot{V})$ can be represented as $\mathbf{F}(\mathbf{S}, V)$. Note that, given $V(t)$, the state-space equations (30) can be solved for a unique $\mathbf{S}(V)$. Therefore, $\tilde{J} = \tilde{J}(V)$ is a unique function of $V(t)$. Let H denote the Hamiltonian function as

$$H(\mathbf{S}, \boldsymbol{\lambda}, V) = \boldsymbol{\lambda}^{\mathrm{T}}(t) \mathbf{F}(\mathbf{S}, V) \tag{45}$$

where $\boldsymbol{\lambda}(t)$ is a $2N^2$-dimensional vector including adjoint variables. The necessary optimality conditions are as follows [31]:

$$\dot{\boldsymbol{\lambda}}(t) = -\partial H / \partial \mathbf{S} = -\mathbf{A}(t) \boldsymbol{\lambda}(t) \tag{46}$$

$$\boldsymbol{\lambda}(t_f) = [\mathbf{Q}(t_f) + \mathbf{W}] \mathbf{S}(t_f). \tag{47}$$

Then, the gradient is

$$g(t) = \partial H / \partial V = \boldsymbol{\lambda}^{\mathrm{T}}(t) [\mathbf{B}_1 + 2V \mathbf{B}_2 + d_v \mathbf{B}_3] \mathbf{S}(t). \tag{48}$$

The CG direction of $V(t)$ in the kth iteration is determined as

$$p_k(t) = -g_k(t) + \beta_k p_{k-1}(t) \tag{49}$$

where

$$\beta_k = \int_0^{t_f} g_k^2(t) dt \Big/ \int_0^{t_f} g_{k-1}^2(t) dt \tag{50}$$

and

$$g_k(t) = (\partial H / \partial V)|_k. \tag{51}$$

Let $V_k(t)$ be the kth approximation to the proposed velocity profile. A new estimate of $V(t)$ is

$$V_{k+1}(t) = V_k(t) + \alpha_k p_k(t) \tag{52}$$

where α_k is chosen to minimize $\tilde{J}(V_k + \alpha_k p_k)$. The technique to search α_k is given in [32, Sec. 7]. The convergence of the CG algorithm is presented in [31].

Profile Design: The proposed control design using the CG algorithm to generate the proposed velocity profile is summarized as follows.

Step 1) t_f, $\mathbf{S}_0$, and V_0 are given. Set $k = 0$.

Step 2) Solve the state-space equation (30) forwards with $V = V_k$ and the adjoint equations (46) and (47) backwards, and then compute p_k from (49). If $k = 0$, then $p_0 = -g_0$.

Step 3) Choose α_k to minimize $\tilde{J}(V_k + \alpha_k p_k)$. Set $V_{k+1}(t) = V_k(t) + \alpha_k p_k(t)$. If $V_{k+1}(t) < 0$ then $V_{k+1}(t) = 0$.

Step 4) Repeat Steps 2 and 3 until

$$|\tilde{J}(V_{k+1}) - \tilde{J}(V_k)| < \delta \tilde{J}(V_k) \tag{53}$$

where δ is a specified positive number. If the condition (53) holds, then go to Step 5.

Step 5) If $V = 0$, stop; otherwise, set $\mathbf{S}_k \to \mathbf{S}_0$ and $V_k \to V_0$. Go to Step 1.

Remark 7: Using Profile Design, which is based on the CG algorithm, it is guaranteed that the optimal value of the cost function $\tilde{J}^* = 0$ is achieved at t_f. However, it is possible that the axial transport velocity reaches the zero value before the optimal

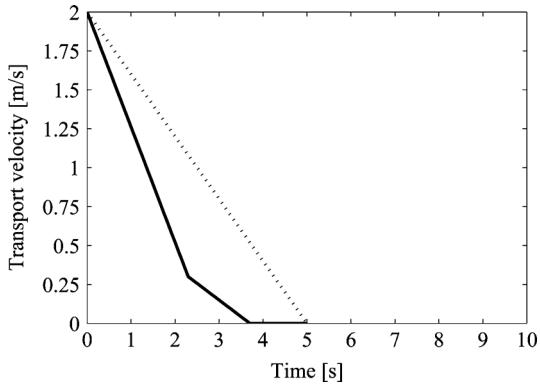

Fig. 5. Comparison of the proposed deceleration profile (solid line) and the conventional constant-deceleration profile (dotted line) in the presence of viscous damping $d_v = 0.001$ N·m^{2}s.

value of the cost function is achieved. The strong technical advantage of the proposed control algorithm is that the vibration energy is assured to be suppressed completely within the deceleration time of the axial transport velocity, in which deceleration time can be selected by the designer.

IV. Simulation Results

Numerical simulations were carried out with the system parameters listed in Table I. The Galerkin method was applied to obtain (25) and (26) with the number of basis functions of the approximate solution $N = 4$. Fig. 5 shows the two profiles for regulation of the axial transport velocity. In this simulation, the axial transport velocity decreased from the value of 2 m/s to zero with a deceleration time of 5 s. In the case of no vibration control, the conventional constant-deceleration velocity profile (dotted line), which has only a slope, was used. Meanwhile, the proposed velocity profile (solid line) generated by using Profile Design was composed of 3 slopes. The optimal control problem was solved with the terminal time $t_f = 5$, and the proposed velocity profile was obtained with 57 iterations of the CG algorithm. The weight coefficient matrix was chosen as $\mathbf{W} = \mathbf{I}$, where $\mathbf{I}$ is the identity matrix.

In this brief, the approximate dynamic model (25)–(26) was used only to design the proposed velocity profile. For numerical simulations to demonstrate the suppression of the transverse displacement, the finite difference method was employed to find an approximate solution for the PDE (13) with the boundary conditions given by (14)–(16) and the time-varying velocity provided by the profiles as shown in Figs. 5 and 7. It should be noted that the stress functions in (13) are obtained by using (25) as mentioned in Remark 3.

Fig. 6 demonstrates the dynamic responses of the axially moving membrane to two time-varying transport velocities (the proposed and the conventional constant-deceleration profiles). As shown in Fig. 6(a), the vibration energy decays to zero in both cases. However, the convergence properties are different. In the control case (the proposed profile is used), the vibration energy (solid line) approaches the zero value at the time $t = 5$; that is, the transverse vibration is suppressed completely within the deceleration time, as the control objective mentioned. This

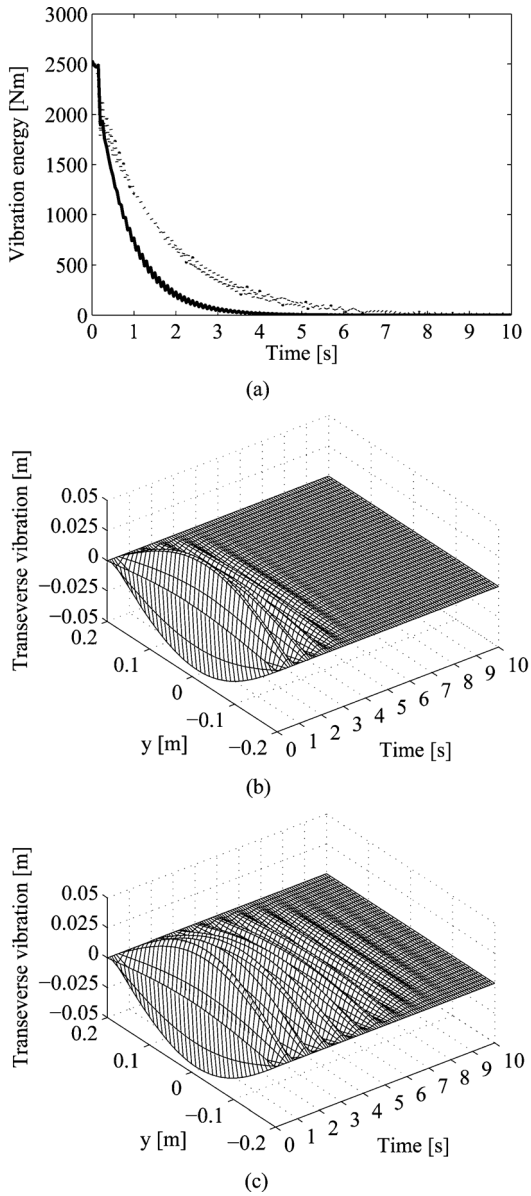

Fig. 6. Comparison of the vibration energies and the transverse displacements in the presence of viscous damping $d_v = 0.001$ N·m^{2}s. (a) Convergence of the vibration energies: controlled (solid line) versus uncontrolled (dotted line). (b) Convergence of the transverse displacement at $x = l/2$ (with control). (c) Slow convergence of the transverse displacement at $x = l/2$ (without control).

is consistent with the theoretical point inferred in Remark 7. In this case, when the axial transport velocity (solid line) reaches zero at the time $t = 3.7, E(3.7) = 16$. After the axial transport velocity reaches zero, the residual vibration energy converges slowly to zero within 1.3 s. From the physical point of view, as mentioned in Section III, plenty of time is required if the transverse vibration is suppressed by only the viscous damping force. Therefore, the residual vibration energy should approach a small value when the axial transport velocity reaches zero. In this brief, this control strategy was executed using the CG method. The theoretical basis of the application of the CG method is that the vibration energy decays most quickly between two consecutive iterations of the CG algorithm. As shown in Fig. 6(a), this theoretical point was verified. In the

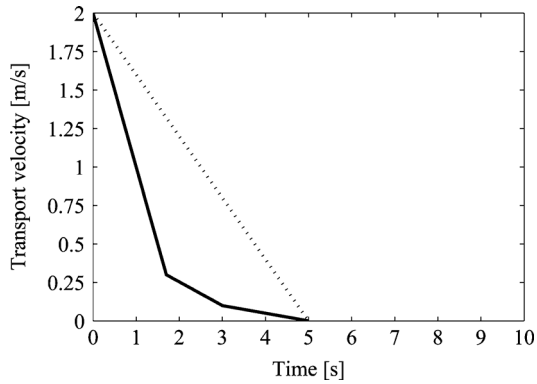

Fig. 7. Deceleration profile generated from the proposed method (solid line) when viscous damping does not exist.

case of control, comparing $E(0) = 2500$ and $E(3.7) = 16$, it can be concluded that the vibration energy is almost suppressed when the axial transport velocity reaches zero.

In the case of no control, it seems that the convergence speed of the vibration energy (dotted line) does not change during the deceleration time. According to the conventional constant-deceleration profile, suppression of the vibration energy takes 9 seconds. Moreover, when the axial transport velocity reaches zero at $t = 5$, the value of the residual vibration energy is considerable $(E(5) = 66)$. It was shown that the vibration energy in the case of no vibration control decays more slowly than in the case of vibration control, especially when the axial transport velocity decreases from the initial value to zero. The convergences of the transverse displacements of the axially moving membrane at $x = l/2$ to zero in the two cases (with control and without control) were compared, as shown in Fig. 6(b) and (c), respectively.

In practice, a number of web materials such as films and textiles may possess very small viscous damping, which can be assumed to be zero $(d_v = 0)$. This leads to that the residual transverse vibration may not be suppressed without control. In this case, the proposed control method is well suitable for the R2R systems which are similar to the R2R lithography system presented in Section I, where the conventional vibration controls, boundary and distributed controls, are not be able to be employed. This will be verified by numerical simulations, as shown in Fig. 8. The system parameters (except the viscous damping coefficient) were maintained as presented in Table I. The axial velocity profile for vibration suppression (solid line) was proposed as shown in Fig. 7. The simulation results shown in Fig. 8 indicate that the vibration energy (dotted-line) cannot converge to zero without the presence of a viscous damping force, when the conventional constant-deceleration profile is used. Meanwhile, the transverse vibration was suppressed completely by the regulation of the axial transport velocity using the proposed profile (solid-line). Through a comparison of the simulation results (time of vibration suppression and control performance) for control and no control, the considerable improvement effected by applying the control algorithm to the membrane system for vibration suppression was verified.

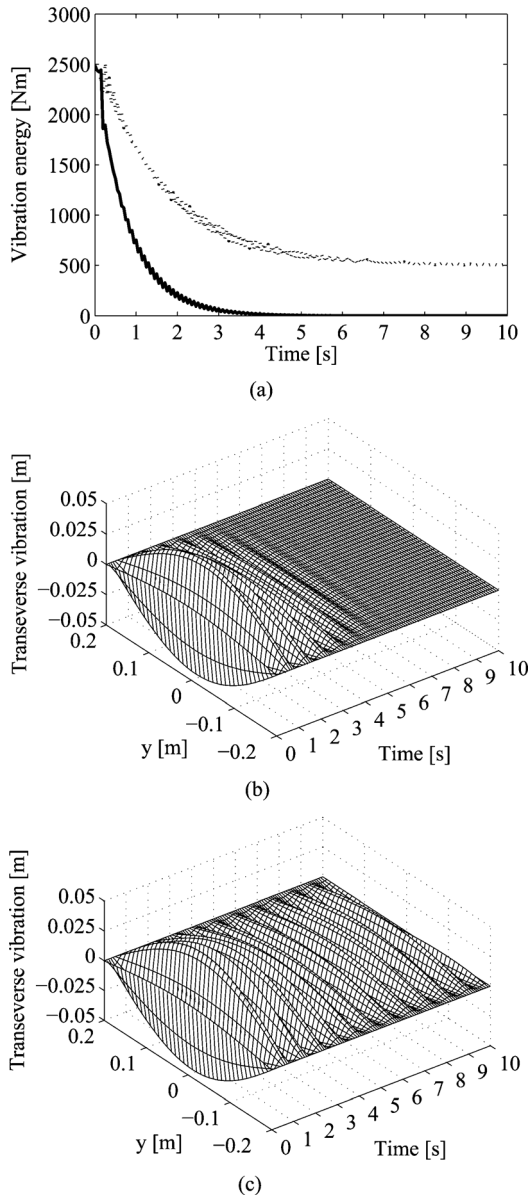

Fig. 8. Comparison of the vibration energies and the transverse displacements in the case of no viscous damping. (a) Convergence of the vibration energies: controlled (solid line) versus uncontrolled (dotted line). (b) Convergence of the transverse displacement at $x = l/2$ (with control). (c) Non-converging transverse displacement at $x = l/2$ due to no viscous damping (without control).

TABLE I
SYSTEM PARAMETERS USED IN SIMULATIONS

Parameter	Description	Value
ρ	Mass density	1.17×10^3 kg/m^3
E	Young's modulus	1.8×10^7 N/m^2
l	Distance between two rolls	4 m
b	Width of the membrane	0.4 m
h	Thickness of the membrane	0.0015 m
d_v	Viscous damping coefficient	0.001 N·m^{2}s
P_0	Initial tension per unit width	400 N/m
V_0	Initial axial velocity	5 m/s
$u_0(x,y)$	Initial longitudinal displacement	0
$v_0(x,y)$	Initial lateral displacement	0
$w_0(x,y)$	Initial transverse displacement	$0.05\sin(\pi x/l)\sin(\pi y/b)$
$w_{t0}(x,y)$	Initial transverse velocity	0

V. Conclusion

In this brief, a novel control algorithm that uses the effects of the time-varying axial transport velocity to suppress the transverse vibration of an axially moving membrane was developed. The basis of the proposed control algorithm is the regulation of the axial transport velocity to track the proposed profile according to which the vibration energy decays most quickly. With regard to the dynamics of the axially moving membrane, the Galerkin method was applied to reduce PDEs into sets of ODEs, which were rewritten into state-space equations. A design procedure based on the CG method was introduced to generate the proposed velocity profile. Compared with the case of no control, the proposed control algorithm provided considerably improved suppression of the vibration energy. It is believed that the proposed control algorithm is the first work using the regulation of the axial transport velocity to suppress the transverse vibration of an axially moving system. This is also expected to provide a feasible solution to problem of the vibration control of axially moving systems when the application of boundary control technique is impossible.

References

[1] K. Jain, M. Klosner, and M. Zemel, "Flexible electronics and displays: High-resolution, roll-to-roll, projection lithography and photoablation processing technologies for high-throughput production," *Proc. IEEE*, vol. 93, no. 8, pp. 1500–1510, Aug. 2005.

[2] M. Pakdemirli, A. G. Ulsoy, and A. Ceranoglu, "Transverse vibration of an axially moving accelerating string," *J. Sound Vib.*, vol. 169, no. 2, pp. 179–196, 1994.

[3] A. E. Jain and A. J. Pritchard, "Sensors and actuators in distributed systems," *Int. J. Control*, vol. 46, no. 4, pp. 1139–1153, 1987.

[4] R.-F. Fung, J. W. Wu, and S. L. Wu, "Exponential stabilization of an axially moving string by linear boundary feedback," *Automatica*, vol. 35, pp. 177–181, 1999.

[5] Y. Li and C. D. Rahn, "Adaptive vibration isolation for axially moving beams," *IEEE/ASME Trans. Mechatron.*, vol. 5, no. 4, pp. 419–428, Dec. 2000.

[6] W. D. Zhu and J. Ni, "Energetics and stability of translating media with an arbitrary varying length," *ASME J. Vib. Acoust.*, vol. 122, no. 3, pp. 295–304, 2000.

[7] Z. Qu, "Robust and adaptive boundary control of a stretched string on a moving transporter," *IEEE Trans. Autom. Control*, vol. 46, no. 3, pp. 1045–1054, Mar. 2001.

[8] K.-J. Yang, K.-S. Hong, and F. Matsuno, "Robust adaptive boundary control of an axially moving string under a spatiotemporally varying tension," *J. Sound Vib.*, vol. 273, no. 4–5, pp. 1007–1029, 2004.

[9] J. Y. Choi, K.-S. Hong, and K.-J. Yang, "Exponential stabilization of an axially moving tenstioned strip by passive damping and boundary control," *J. Vib. Control*, vol. 10, no. 5, pp. 661–682, 2004.

[10] K.-J. Yang, K.-S. Hong, and F. Matsuno, "Energy-based control of axially translating beams: Varying tension, varying speed, and disturbance adaptation," *IEEE Trans. Control Syst. Technol.*, vol. 13, no. 6, pp. 1045–1054, Nov. 2005.

[11] Q. H. Ngo, K.-S. Hong, and I. H. Jung, "Adaptive control of an axially moving system," *J. Mech. Sci. Technol.*, vol. 23, no. 11, pp. 3071–3078, 2009.

[12] B. V. E. How, S. S. Ge, and Y. S. Cho, "Active control of flexible marine risers," *J. Sound Vib.*, vol. 320, no. 4–5, pp. 758–776, 2009.

[13] Q. C. Nguyen and K.-S. Hong, "Asymptotic stabilization of a nonlinear axially moving string by adaptive boundary control," *J. Sound Vib.*, vol. 329, no. 22, pp. 4588–4603, 2010.

[14] S. S. Ge, W. He, B. V. E. How, and Y. S. Choo, "Boundary control of a coupled nonlinear flexible marine riser," *IEEE Trans. Control Syst. Technol.*, vol. 16, no. 5, pp. 1080–1091, Sep. 2010.

[15] R. Vazquez and M. Krstic, "Boundary observer for output-feedback stabilization of thermal-fluid convection loop," *IEEE Trans. Control Syst. Technol.*, vol. 18, no. 4, pp. 789–797, Jul. 2010.

[16] A. Smyshlyaev, T. Meurer, and M. Krstic, "Further results on stabilization of shock-like equilibria of the viscous burgers PDE," *IEEE Trans. Autom. Control*, vol. 55, no. 8, pp. 1942–1946, Aug. 2010.

[17] W. He, S. S. Ge, B. V. E. How, Y. S. Choo, and K.-S. Hong, "Robust adaptive boundary control of a flexible marine riser with vessel dynamics," *Automatica*, vol. 47, no. 4, pp. 722–732, 2011.

[18] W. He and S. S. Ge, "Robust adaptive boundary control of a vibrating string under unknown time-varying disturbance," *IEEE Trans. Control Syst. Technol.*, 10.1109/TCST.2010.2099230.

[19] I. Tunay, S. Y. Yoon, and K. Woerner, "Vibration analysis and control of magnet positioned using curved-beam models," *IEEE Trans. Control Syst. Technol.*, vol. 17, no. 5, pp. 1415–1423, Sep. 2009.

[20] D. Bandopadhya and J. Njuguna, "A study on the effects of Kalman filter on performance of IPMC-based active vibration control scheme," *IEEE Trans. Control Syst. Technol.*, vol. 18, no. 6, pp. 1315–1324, Nov. 2010.

[21] Q. H. Ngo and K.-S. Hong, "Sliding mode anti-sway control of an offhose container crane," *IEEE/ASME Trans. Mechatron.*, 10.1109/TMECH.2010.2093907.

[22] Q. C. Nguyen and K.-S. Hong, "Stabilization of an axially moving web via regulation of axial velocity," *J. Sound Vib.*, 10.1016/j.jsv.2011.04.029.

[23] H. R. Oz, M. Pakdemirli, and H. Boyacı, "Non-linear vibrations and stability of an axially moving beam with time-dependent velocity," *Int. J. Non-Linear Mech.*, vol. 36, no. 1, pp. 107–115, 2001.

[24] F. Pellicano, G. Catellani, and A. Fregolent, "Parametric instability of belts: Theory and experiments," *Comput. Structures*, vol. 82, no. 1, pp. 81–91, 2004.

[25] C. Shin, J. Chung, and W. Kim, "Dynamic characteristics of the out-of-plane vibration for an axially moving membrane," *J. Sound Vib.*, vol. 286, no. 4–5, pp. 1019–1031, 2005.

[26] C. Shin, J. Chung, and H. H. Yoo, "Dynamics responses of the in-plane and out-of-plane vibrations for an axially moving membrane," *J. Sound Vib.*, vol. 297, no. 3–5, pp. 794–809, 2006.

[27] S. V. Ponomareva and W. T. van Horssen, "On transversal vibration of an axially moving string with a time-varying velocity," *Nonlinear Dyn.*, vol. 37, no. 1–2, pp. 315–323, Jan. 2007.

[28] A. Bazaei and M. Moallem, "Force transmission through a structurally flexible beam: Dynamic modeling and feedback control," *IEEE Trans. Control Syst. Technol.*, vol. 17, no. 6, pp. 1245–1256, Nov. 2009.

[29] H. Ding and L.-Q. Chen, "Galerkin methods for natural frequencies of high-speed axially moving beams," *J. Sound Vib.*, vol. 329, no. 17, pp. 3484–3494, 2010.

[30] M. R. Kermani, "Analytic modal analyses of a partially strengthened Timoshenko beam," *IEEE Trans. Control Syst. Technol.*, vol. 18, no. 4, pp. 850–858, Jul. 2010.

[31] L. S. Lasdon, S. K. Mitter, and A. D. Waren, "The conjugate gradient method for optimal control problems," *IEEE Trans. Autom. Control*, vol. AC-12, no. 2, pp. 132–138, Apr. 1967.

[32] J. C. Heideman and A. V. Levy, "Sequential conjugate-gradient-restoration algorithm for opitimal control problems. Part1. Theory," *J. Optim. Theor. Appl.*, vol. 15, no. 2, pp. 203–222, 1975.